Seppälä A. 2001. Some improvements to the approximate analytical solution of the problem of laminar flow between permeable and impermeable wall. Acta Polytechnica Scandinavica, Mechanical Engineering Series 152: 1-21.

Me 152

ACTA POLYTECHNICA SCANDINAVICA

MECHANICAL ENGINEERING SERIES No. 152

Some Improvements to the Approximate Analytical Solution of the Problem of Laminar Flow between Permeable and Impermeable Wall

ARI SEPPÄLÄ

Helsinki University of Technology
Department of Mechanical Engineering
Laboratory of Applied Thermodynamics
P.O.Box 4100
FIN-02015 HUT
Finland

ESPOO 2001

Seppälä, Ari, **Some improvements to the approximate analytical solution of the problem of laminar flow between permeable and impermeable wall.** Acta Polytechnica Scandinavica, Mechanical Engineering Series No. 152, Espoo 2001, 21 pp. Published by the Finnish Academies of Technology. ISBN 951-666-580-2, ISSN 0001-687X.

Keywords: fluid mechanics, porous wall, slip condition, perturbation method

Abstract

The two-dimensional Navier-Stokes equations for steady, laminar, incompressible fluid flow between a non-porous and porous wall are solved up to second order perturbation approximation. An external constant force term, perpendicular to the porous wall, is added to the Navier-Stokes equation and the pressure change equations in both directions are solved. The accuracy of zero-, first- and second-order approximations has been studied up to the 20th order.

Nomenclature

A	surface area, m^2
h	channel height, m
k	constant of integration
k_p	permeability, m^2
L	length , m
p	hydrostatic pressure, Pa
Re_w	wall Reynolds number, dimensionless
u	velocity of the solution inside the channel, tangential to the porous wall, m/s
u_{slip}	tangential (slip) velocity on the surface of porous wall, m/s
u_m	mean velocity at cross-sectional area of channel, m/s
v	velocity of the solution inside the channel, normal to the porous wall, m/s
v_w	permeating flow through the porous wall, m^3/m^2s
W	channel width, m
x	co-ordinate, in tangential to the porous wall
y	co-ordinate, in normal direction to the porous wall
α	coefficient in slip coefficient, dimensionless
λ	dimensionless co-ordinate (= y/h)
μ	dynamic viscosity, Ns/m^2
ν	kinematic viscosity, m^2/s
∂	partial differential
Θ	dimensionless slip coefficient
Θ'	slip coefficient, m
$\Im$	external force, N/m^3

1. Introduction

Velocity profiles and pressure change equations of two-dimensional laminar steady state fluid flow between a permeable and impermeable wall are solved. The flux through the permeable wall is assumed to be independent of position. The fluid is assumed incompressible and the kinematic viscosity (ν) is considered as constant. The study is restricted into small values of wall Reynolds numbers. The solution follows the studies of Berman [1] and Chellam et al. [2]. Berman first studied the same case but with two equally permeable walls. Chellam et al. solved the same problem with one impermeable and one permeable wall with a slip condition and studied especially the effect of the slip on the problem. In the present study some improvements for the solution of the problem are reported. The studies of Berman and Chellam et al. were based on a guessed form of stream function. In this study, an alternative approach to the derivation of the forms of velocity profiles is given. Secondly, we give the solution for the pressure change perpendicular to the channel walls in the case of one permeable wall with the slip condition. In addition to the studies of Berman and Chellam et al., an constant external force term perpendicular to the permeable wall is included into the study. Furthermore, the second order perturbation solution for the velocity profiles is given and a sufficient order of approximation is studied up to the 20th order (previously studied only to the 2nd order).

The results can be utilised, for example, in estimating the concentration profiles of solution flow inside a channel (with a rectangular cross-section) affected by the flux through the permeable wall.

2. Fundamental equations and boundary conditions

The co-ordinate system (Figure 1) is chosen with its origin at the surface of the impermeable wall. The y-axis, which is perpendicular to the channel walls, is transformed into dimensionless variable

$$\lambda = y/h \tag{1}$$

where h is the distance between the walls (channel height).

The continuity equation for the problem can be written as

$$\frac{\partial u}{\partial x} + \frac{1}{h}\frac{\partial v}{\partial \lambda} = 0 \tag{2}$$

where $u = u(x,\lambda)$ is the velocity component in the x- direction and $v = v(x,\lambda)$ is the velocity component in the λ-direction. The Navier-Stokes equations of motion are

$$u\frac{\partial u}{\partial x} + \frac{v}{h}\frac{\partial u}{\partial \lambda} = -\frac{1}{\rho}\frac{\partial p}{\partial x} + \nu\left[\frac{\partial^2 u}{\partial x^2} + \frac{1}{h^2}\frac{\partial^2 u}{\partial \lambda^2}\right] \tag{3}$$

$$u\frac{\partial v}{\partial x} + \frac{v}{h}\frac{\partial v}{\partial \lambda} = \frac{1}{\rho}\Im_\lambda - \frac{1}{\rho h}\frac{\partial p}{\partial \lambda} + \nu\left[\frac{\partial^2 v}{\partial x^2} + \frac{1}{h^2}\frac{\partial^2 v}{\partial \lambda^2}\right] \tag{4}$$

where p is the hydrostatic pressure, $\Im_\lambda$ the external force in the direction of λ, ν the kinematic viscosity and ρ the density of the fluid.

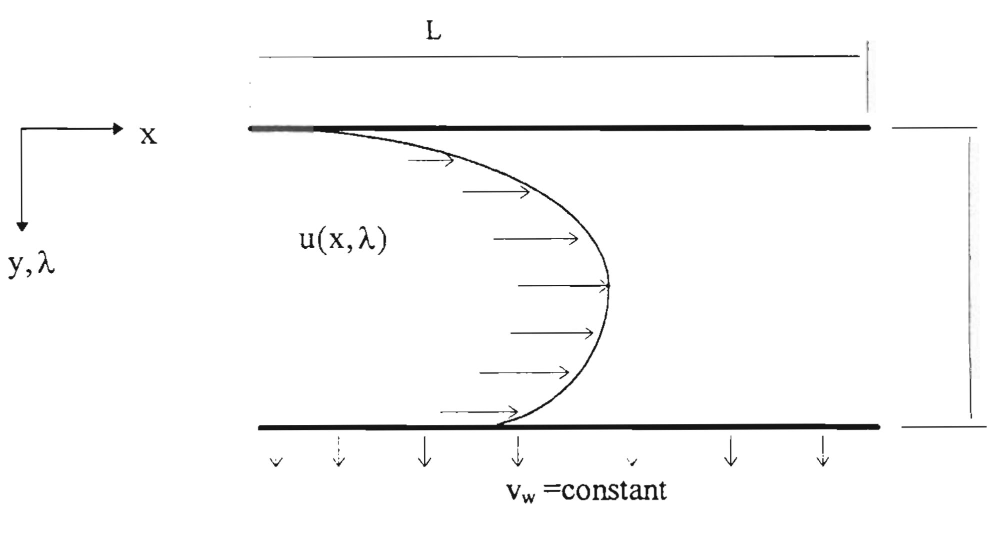

Figure 1. Two dimensional flow in a channel of rectangular cross section with one permeable wall.

The boundary conditions are

$$u(x,0) = 0 \tag{5a}$$

$$u(x,1) = u_{slip} = -\Theta'\frac{\partial u}{\partial y} + O(k_p) = -\Theta\frac{\partial u}{\partial \lambda} + O(k_p) \tag{5b}$$

$v(x,0) = 0$ (6a)

$v(x,l) = v_w = \text{constant}$ (6b)

Eq. (5b) is the slip-boundary condition, suggested by Beavers and Joseph [3] and Saffman [4] for the permeable wall. The coefficient $\Theta' = \frac{k_p^{1/2}}{\alpha}$ so that the slip coefficient Θ can be expressed as a function of the permeability (k_p) of porous wall, of the dimensionless constant (α) and of the channel height (h) as

$$\Theta = \frac{k_p^{1/2}}{\alpha h} \tag{7}$$

The correction term ($O(k_p)$) has been omitted from this study.

3. Form of the steady-state velocity profiles

The velocity profiles are assumed to achieve separated solutions i.e.

$$u(x,\lambda) = G(x)F(\lambda) \tag{8}$$

$$v(x,\lambda) = g(x)f(\lambda) \tag{9}$$

Since the flux through the permeable boundary ($\lambda = 1$) is assumed constant, the mean velocity in the x-direction, $u_m = u_m(x)$, changes linearly. Applying Eq. (8) we get for the mean velocity

$$u_m(x) = \frac{\int_0^h u(x,\lambda)d\lambda}{h} = G(x)\frac{\int_0^h F(\lambda)d\lambda}{h} \tag{10}$$

Thus, the function G(x) and so also the velocity $u(x,\lambda)$ are linear in respect of the x-co-ordinate:

$$G = B_1 x + B_2 \tag{11}$$

where B_1 and B_2 are constants.

Assuming constant density, the change of mass flow ($= \rho u_m hW$) inside the channel must equal the permeating mass flow:

$$d(\rho u_m(x)hW) = -\rho v_w W dx \tag{12}$$

where W is the width of the channel.

Using equations (12) and (10) we get, for constant ρ, h, W

$$\frac{du_m(x)}{dx} = -\frac{v_w}{h} = \frac{dG(x)}{dx} \cdot \frac{\int_0^h F(\lambda)d\lambda}{h} \tag{13}$$

Substituting Eqs. (8) - (9) into the continuity equation, Eq. (2), and applying Eq. (11) we get

$$B_1 F(\lambda) + \frac{g(x)}{h}\frac{df(\lambda)}{d\lambda} = 0 \tag{14}$$

This means that

$$g(x) = \text{constant} = B_3 \tag{15}$$

That is the v-velocity becomes independent everywhere of the x-co-ordinate. Applying Eq. (10) at $u_m(x=0) = u_m^0$ (the initial mean velocity), Eqs. (8)-(9), (11), (13) and (14)-(15), we get for the velocities

$$u(x,\lambda) = B_3\left(-\frac{x}{h} + \frac{u_m^0}{v_w}\right)f'(\lambda) \tag{16a}$$

$$v(\lambda) = B_3 f(\lambda) \tag{16b}$$

As f in Eqs. (16a) and (16b) is yet an undetermined function, the constant coefficient B_3 can be freely chosen. We set $B_3 = v_w$, so the velocity profiles are of the form

$$u(x,\lambda) = \left(-\frac{v_w x}{h} + u_m^0\right)f'(\lambda) \tag{17}$$

$$v(\lambda) = v_w f(\lambda) \tag{18}$$

which is exactly the same result that Berman [1] found for the case of two equally permeable walls (in this case the λ-axis is placed at the midway between the planes.) and Chellam et al. [2] for one porous and one non-porous walls. However, studies [1]-[2] were based on the assumed form of stream function Ψ

$\Psi(x,\lambda) = (hu_m^0 - v_w x)f(\lambda)$.

4. Solution of the velocity profiles

When Eqs. (17) and (18) are substituted in the equation of motion (3) - (4), the results are

$$-\frac{1}{\rho}\frac{\partial p}{\partial x}=\left[u_m^0-\frac{v_w x}{h}\right]\left[-\frac{v_w}{h}\left(f'^2-f\ f''\right)-\frac{\nu}{h^2}f'''\right] \tag{19}$$

$$-\frac{1}{h\rho}\frac{\partial p}{\partial \lambda}=\frac{v}{h}\frac{dv}{d\lambda}-\frac{\nu}{h^2}\frac{d^2v}{d\lambda^2}-\frac{1}{\rho}\Im_\lambda \tag{20}$$

Differentiating Eq. (20) with respect to x results in (when $\Im_\lambda$ is independent of x)

$$\frac{\partial^2 p}{\partial x \partial y}=0 \tag{21}$$

Differentiating Eq. (19) with respect to λ and applying Eq. (21) results

$$\left[u_m^0-\frac{v_w x}{h}\right]\frac{d}{d\lambda}\left[\frac{v_w}{h}\left(f'^2-f\ f''\right)+\frac{\nu}{h^2}f'''\right]=0 \tag{22}$$

If Eq. (22) is to be satisfied for all x, then

$$\frac{d}{d\lambda}\left[\frac{v_w}{h}\left(f'^2-f\ f''\right)+\frac{\nu}{h^2}f'''\right]=0 \tag{23}$$

Integrating and defining a Reynolds number at the permeable wall, the wall Reynolds number, as

$$Re_w=\frac{v_w h}{\nu} \tag{24}$$

we obtain a third order, non-linear, ordinary differential equation for the unknown function f:

$$Re_w\left(f'^2-f\ f''\right)+f'''=k \tag{25}$$

where k is the constant of integration.

The boundary condition for solving this equation can be obtained from Eqs. (5a) - (6b) and (17) - (18):

$$f(0)=f'(0)=0 \tag{26a}$$

$$f(1)=1 \tag{26b}$$

$$f'(1)=-\Theta\ f''(1) \tag{26c}$$

Perturbation treatment

The wall Reynolds number, defined in Eq. (24) is used as a perturbation parameter. The study is limited only for sufficiently small values of Re_w. For more details about the parameter perturbation method see e.g. [5]. Expanding the function $f(\lambda)$ and the constant k in power series of Re_w, we get

$$f(\lambda) = f_0(\lambda) + f_1(\lambda) Re_w + f_2(\lambda) Re_w^2 + \cdots = \sum_{i=0\ldots} f_i Re_w^i \tag{27}$$

and

$$k = C_0 + C_1 Re_w + C_2 Re_w^2 + \cdots = \sum_{i=0\ldots} C_i Re_w^i \tag{28}$$

where f_i and C_i are independent of Re_w and i in Re_w^i denotes power. Inserting Eq. (27) and Eq. (28) into Eq. (25), and collecting coefficients of equal powers of Re_w results in the equations (from zero order to second order):

$$f_0''' = C_0 \tag{29}$$

$$f_1''' = C_1 + f_0 f_0'' - f_0'^2 \tag{30}$$

$$f_2''' = C_2 + f_0 f_1'' + f_1 f_0'' + 2 f_0' f_1' \tag{31}$$

The boundary conditions, Eq. (26a) -(26c), can now be written as

$$f_i(0) = f_i'(0) = 0; \qquad i \geq 0 \tag{32a}$$

$$f_0(1) = 1 \tag{32b}$$

$$f_i(1) = 0; \qquad i \geq 1 \tag{32c}$$

$$f_i'(1) = -\Theta\ f_i''(1) \qquad i \geq 0 \tag{32d}$$

The zero-, first- and second-order perturbation solutions for the function f are solved from Eqs. (29) - (32). This results in an expression for the function f_i (i=0,1,2)

$$f_i(\lambda) = \sum_{j=2}^{11} a_{i,j} \lambda^j \tag{33}$$

where the j in λ^j denotes power. The coefficients $a_{i,j}$ are shown in Table 1. For example, the velocity profiles resulting from the second-order approximation (with the no-slip condition Θ =0) are

$$u(x,\lambda) = \left(-\frac{v_w x}{h} + u_m^0\right)\cdot$$

$$\left[-6\lambda^2 + 6\lambda + \frac{Re_w}{210}\left(-84\lambda^6 + 252\lambda^5 - 415\lambda^4 + 243\lambda^2 - 96\lambda\right) + \frac{Re_w^2}{323400}\left(2464\lambda^{10} - 12320\lambda^9 + \right.\right.$$

$$\left.\left. 13860\lambda^8 - 13860\lambda^7 + 49896\lambda^6 - 104412\lambda^5 + 73920\lambda^4 - 8787\lambda^2 - 761\lambda\right)\right] \tag{34}$$

$$v(\lambda) = v_w\left[-2\lambda^3 + 3\lambda^2 + \frac{Re_w}{210}\left(-12\lambda^7 + 42\lambda^6 - 63\lambda^5 + 81\lambda^3 - 48\lambda^2\right) + \frac{Re_w^2}{646800}\left(448\lambda^{11} - 2464\lambda^{10} + \right.\right.$$

$$\left.\left. 3080\lambda^9 - 3465\lambda^8 + 14256\lambda^7 - 34804\lambda^6 + 29568\lambda^5 - 5858\lambda^3 - 761\lambda^2\right)\right] \tag{35}$$

An example of the velocity profiles calculated from the second order approximation is illustrated in Fig. 2 for $\Theta = 0.2$. The negative wall Reynolds numbers in Fig. 2 concern a case where the direction of the permeate flux is into the channel, thus causing an increase in the u-velocity. Correspondingly, the positive wall Reynolds numbers concern a case where the permeate flux is out from the channel, causing a decrease in the u-velocity. From the dotted curve of $Re_w = 0.2$ in Fig. 2a, we can see that if the positive wall Reynolds number (or permeate velocity) comes too high in respect of the initial volume flow in the x-direction or the flow path in the x-direction is too long, an non-physical solution (reverted flow) will result. The u-velocity in Fig. 2a is not zero at the permeable wall ($\lambda = 1$) due to the slip effect.

The coefficients C_0, C_1 and C_2 in Eq. (28) are

$$C_0 = -12\frac{(1+\Theta)}{(1+4\Theta)}$$

$$C_1 = \frac{9}{35}\frac{(296\Theta^3 + 272\Theta^2 + 90\Theta + 9)}{(1+4\Theta)^3}$$

$$C_2 = -\frac{1}{53900}\frac{(330144\Theta^5 + 1308952\Theta^4 + 1055644\Theta^3 + 379038\Theta^2 + 55651\Theta + 2929)}{(1+4\Theta)^5}$$

Approximate values of the coefficients C_i, when $\Theta = 0$, are presented in Table 2 up to the 20th order. All of them can be expressed as precise rational numbers. For example

$$C_{10} = \frac{36417229047675069609933303014720617063}{18110776704358680876216687579596307686400000000}.$$

Table 1. The coefficients $a_{i,j}$. The constant $m = 1/646800$.

	i = 0	i = 1	i = 2
j = 2	$3\frac{(1+2\Theta)}{(1+4\Theta)}$	$\frac{-1}{35}\frac{(324\Theta^3+278\Theta^2+88\Theta+8)}{(1+4\Theta)^3}$	$-m\frac{(761+15220\Theta+106120\Theta^2+695264\Theta^3+1928272\Theta^4+2316352\Theta^5)}{(1+20\Theta+160\Theta^2+640\Theta^3+1280\Theta^4+1024\Theta^5)}$
3	$-2\frac{(1+\Theta)}{(1+4\Theta)}$	$\frac{3}{70}\frac{(296\Theta^3+272\Theta^2+90\Theta+9)}{(1+4\Theta)^3}$	$\frac{-2(330144\Theta^5+1308952\Theta^4+1055644\Theta^3+379038\Theta^2+55651\Theta+2929)}{(1+16\Theta+96\Theta^2+256\Theta^3+256\Theta^4)(1+4\Theta)}$
4	0	0	0
5	0	$\frac{-3}{10}\frac{(1+2\Theta)^2}{(1+4\Theta)^2}$	$\frac{29568+384384\Theta+1677984\Theta^2+3252480\Theta^3+2395008\Theta^4}{1+16\Theta+96\Theta^2+256\Theta^3+256\Theta^4}$
6	0	$\frac{1}{5}\frac{(1+2\Theta)(1+\Theta)}{(1+4\Theta)^2}$	$-m\frac{34804+417648\Theta+1703856\Theta^2+3070144\Theta^3+2040192\Theta^4}{1+16\Theta+96\Theta^2+256\Theta^3+256\Theta^4}$
7	0	$\frac{-2}{35}\frac{(1+\Theta)^2}{(1+4\Theta)^2}$	$m\frac{14256+156816\Theta+573408\Theta^2+899712\Theta^3+468864\Theta^4}{1+16\Theta+96\Theta^2+256\Theta^3+256\Theta^4}$
8	0	0	$-m\frac{124740\Theta^2+34650\Theta+110880\Theta^4+3465+194040\Theta^3}{1+16\Theta+96\Theta^2+256\Theta^3+256\Theta^4}$
9	0	0	$m\frac{3080+27720\Theta+86240\Theta^2+110880\Theta^3+49280\Theta^4}{1+16\Theta+96\Theta^2+256\Theta^3+256\Theta^4}$
10	0	0	$-m\frac{2464+19712\Theta+51744\Theta^2+54208\Theta^3+19712\Theta^4}{1+16\Theta+96\Theta^2+256\Theta^3+256\Theta^4}$
11	0	0	$m\frac{448+3136\Theta+6720\Theta^2+5824\Theta^3+1792\Theta^4}{1+16\Theta+96\Theta^2+256\Theta^3+256\Theta^4}$

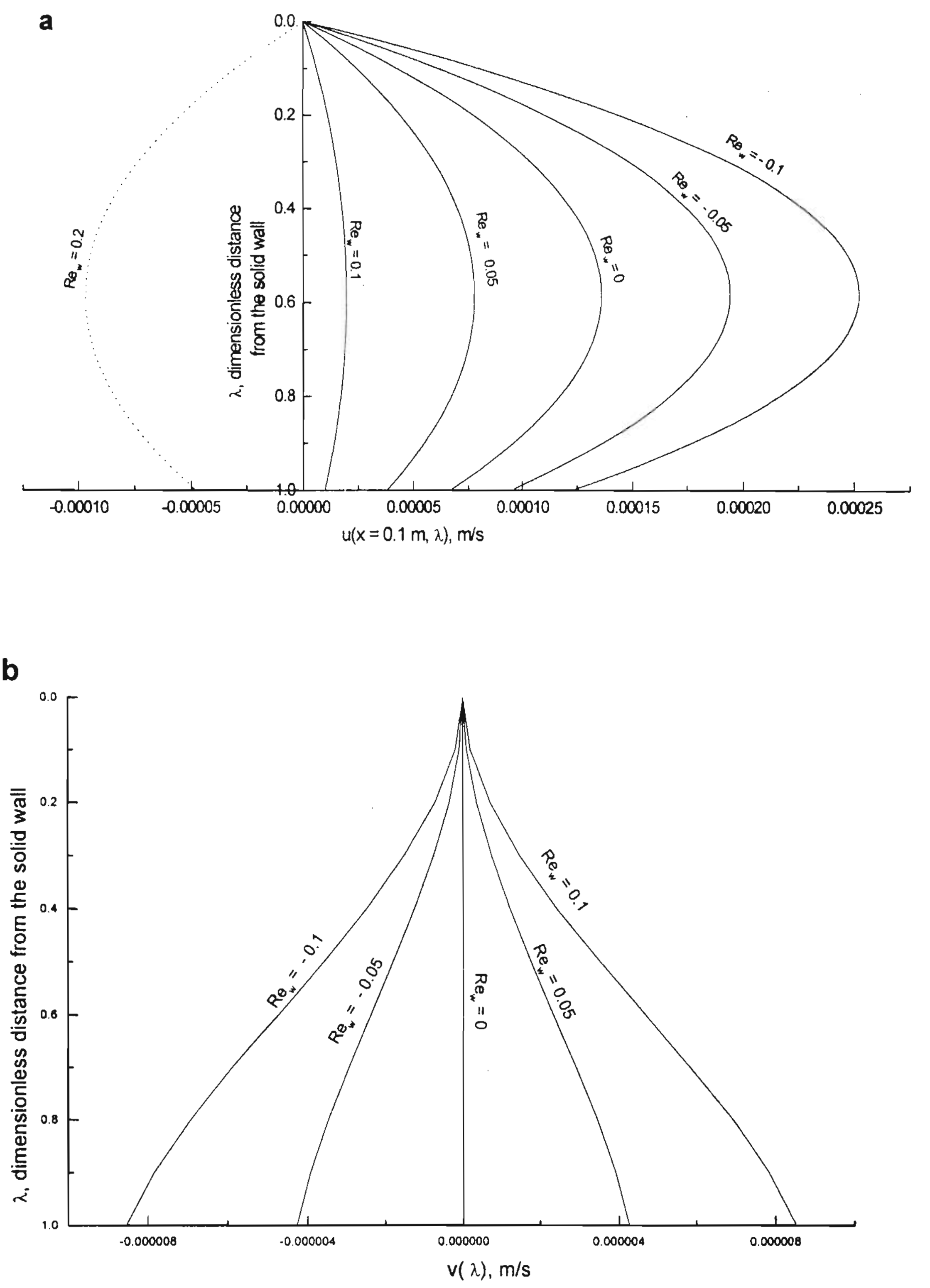

Figure 2. Velocity profiles when h = 10 mm, Θ = 0.2, $\nu = 8.55 \cdot 10^{-4}$ m^2/s (water), $u_m^0 = 0.1$ mm/s.

Table 2. Coefficients C_i for Eq.(28) ($\Theta = 0$).

i	C_i	i	C_i
0	-12	11	$-2.04 \cdot 10^{-12}$
1	2.31	12	$-1.65 \cdot 10^{-13}$
2	-0.054	13	$1.06 \cdot 10^{-14}$
3	$-2.71 \cdot 10^{-3} 0$	14	$1.33 \cdot 10^{-15}$
4	$7.71 \cdot 10^{-5}$	15	$-4.39 \cdot 10^{-17}$
5	$1.47 \cdot 10^{-5}$	16	$-9.92 \cdot 10^{-18}$
6	$9.41 \cdot 10^{-8}$	17	$1.16 \cdot 10^{-19}$
7	$-6.99 \cdot 10^{-8}$	18	$7.22 \cdot 10^{-20}$
8	$-1.69 \cdot 10^{-9}$	19	$6.19 \cdot 10^{-22}$
9	$4.02 \cdot 10^{-10}$	20	$-5.01 \cdot 10^{-22}$
10	$2.01 \cdot 10^{-11}$	-	-

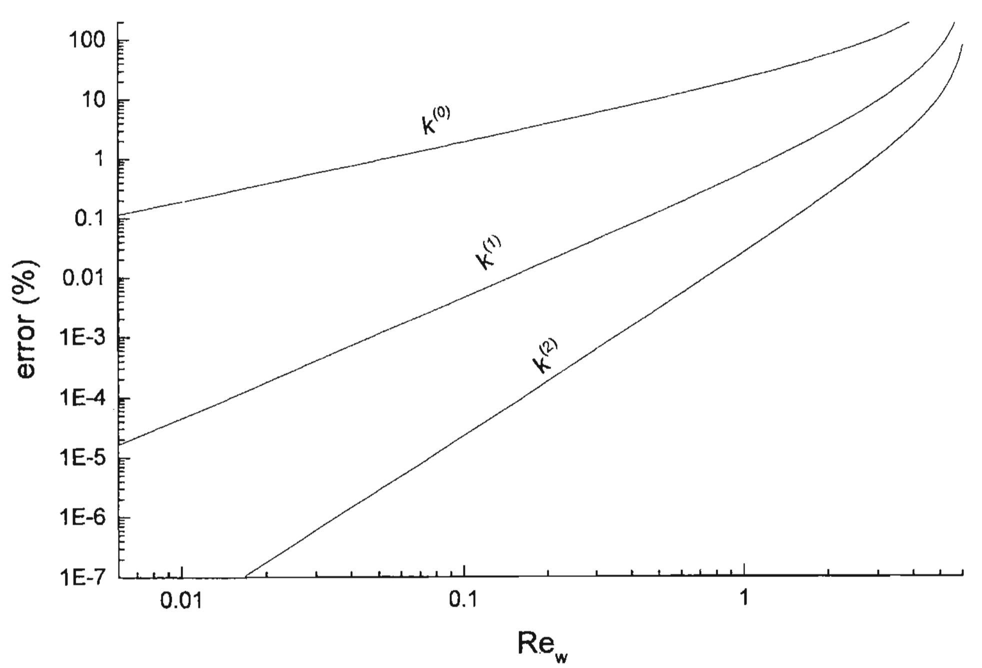

Figure 3. The relative error, $\left|\frac{k^{(n)} - k^{(20)}}{k^{(20)}}\right| \cdot 100\%$, of the zero (n=0), first (n=1) and second order (n=2) perturbation solution of parameter k compared to the 20th order solution.

As can be seen from Table 2, the absolute value of coefficients diminishes continuously, at least up to the 20th order, as the order increases.

The accuracy of the zero- (n=0), first- (n=1) and second-order (n=2) solutions is presented in Fig. 3. We can see that if $Re_w << 1$, the first order approximation is sufficient. For $Re_w << 0.01$ even the zero order approximation results only in a minor error. For values $Re_w = 1$ and a little below, higher order solutions may be needed. However, it has not been shown that the coefficients C_i decrease continuously as the order of solution approaches infinity, although the decrease seems probable according to the values in Table 2. The convergence of the series near $Re_w = 1$ is therefore not properly guaranteed.

5. Pressure change

Applying Eqs. (24) and (25), Eq. (19) can be put into the form

$$\frac{\partial p}{\partial x} = \frac{k\mu}{h^2}\left[u_m^0 - \frac{v_w x}{h}\right] \tag{36}$$

where $\mu = \rho\nu$ is the dynamic viscosity.

Integrating Eq. (36) at the fixed position $\lambda = \lambda_0$ results in a pressure change in the x-direction

$$p(x,\lambda_0) - p(0,\lambda_0) = \frac{k\mu}{h^2}\left[u_m^0 x - \frac{v_w x^2}{2h}\right] \tag{37}$$

The zero-, first- or second order approximation of Eq. (37) can be found by substituting the coefficients C_i into the equation of constant k. Applying Eq. (28) and (37) to an unperturbed case ($Re_w = 0$, $v_w = 0$) results in a pressure drop in the x-direction

$$\frac{\partial p}{\partial x} = \frac{-12\mu}{h^2} u_m^0$$

which is, as it should be, the solution for fully-developed laminar flow between two parallel walls.

The effect of the permeate flux on the pressure drop in the x-direction, described by Eq. (37), is shown in Fig. 4. At the vertical axis, the ratio between the pressure drop in the case $0 < Re_w \leq 1$ and in the case $Re_w = 0$ (fully developed condition) is given as a function of distance from the entrance.

The pressure change in the λ-direction, obtained from Eq. (20) can be written in the form

$$p(x,\lambda) - p(x,\lambda_0) = h\int_{\lambda_0}^{\lambda} \Im_\lambda d\lambda - \rho v_w^2 \sum_{i=1}^{14} d_i(\lambda^i - \lambda_0^i) \tag{38}$$

where i in λ^i denotes power and the coefficients d_i are

$$d_{14} = \frac{a_7^2}{2} Re_w^2$$

$$d_{13} = a_6 a_7 Re_w^2$$

$$d_{12} = a_5 a_7 Re_w^2 + \tfrac{1}{2} a_6^2 Re_w^2$$

$$d_{11} = a_5 a_6 Re_w^2$$

$$d_{10} = \tfrac{7}{10}(b_3 + Re_w a_3) Re_w a_7 + \tfrac{3}{10} Re_w a_7 (b_3 + Re_w a_3) + \tfrac{1}{2} Re_w^2 a_5^2$$

$$d_9 = \tfrac{7}{9}(b_2 + Re_w a_2) Re_w a_7 + \tfrac{2}{3} Re_w a_6 (b_3 + Re_w a_3) + \tfrac{1}{3} Re_w a_6 (b_3 + Re_w a_3) + \tfrac{2}{9} Re_w a_7 (b_2 + Re_w a_2)$$

$$d_8 = \tfrac{3}{4}(b_2 + Re_w a_2) Re_w a_6 + \tfrac{5}{8} Re_w a_5 (b_3 + Re_w a_3) + \tfrac{3}{8} Re_w a_5 (b_3 + Re_w a_3) + \tfrac{1}{4} Re_w a_6 (b_2 + Re_w a_2)$$

$$d_7 = \tfrac{2}{7}(b_2 + Re_w a_2) Re_w a_5 + \tfrac{5}{7} Re_w a_5 (b_2 + Re_w a_2)$$

$$d_6 = -7a_7 + \tfrac{1}{2}(b_3 + Re_w a_3)^2$$

$$d_5 = -6a_6 + (b_2 + Re_w a_2)(b_3 + Re_w a_3)$$

$$d_4 = -5a_5 + \tfrac{1}{2}(b_2 + Re_w a_2)^2$$

$$d_3 = 0$$

$$d_2 = -\frac{3(a_3 Re_w + b_3)}{Re_w}$$

$$d_1 = -\frac{2(a_2 Re_w + b_2)}{Re_w}$$

The Equation (38) can be simplified to the following form if we study the change between the wall surfaces when the slip coefficient is zero

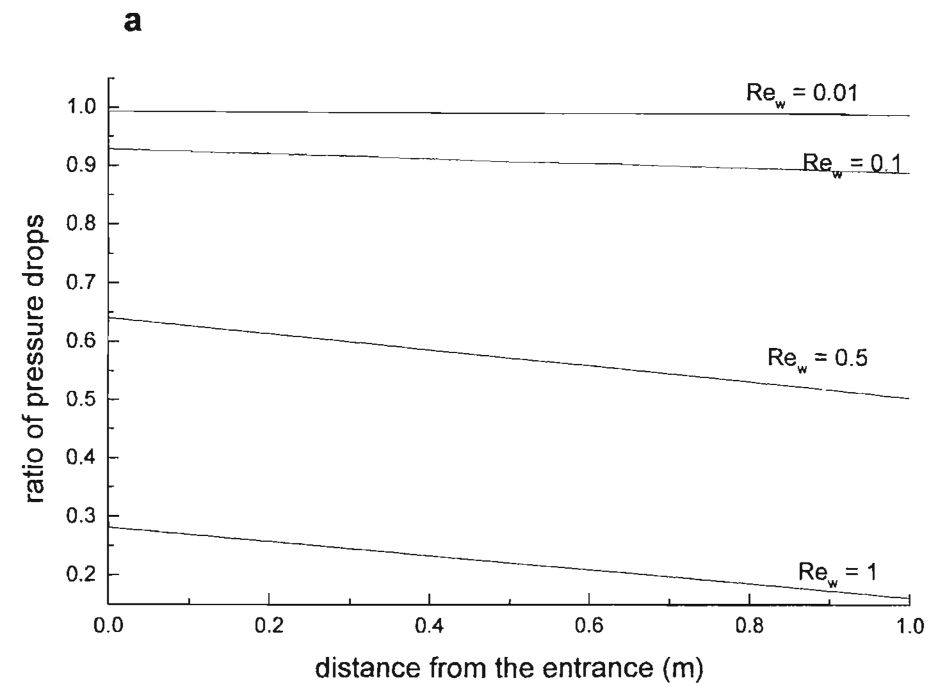

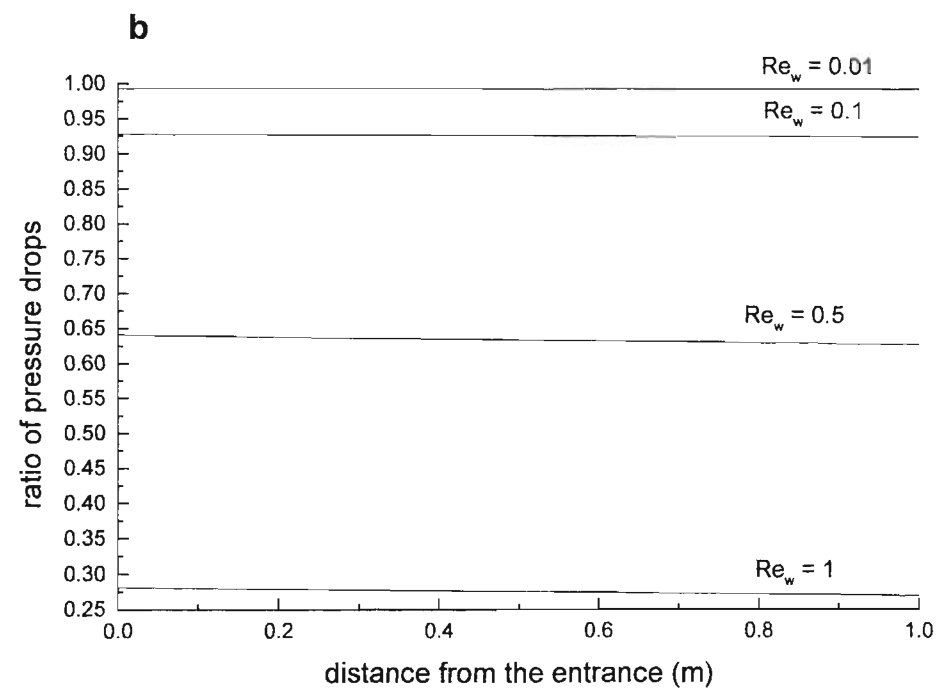

Figure 4. The effect of permeate flux on the pressure change the in x-direction. The ratio is given as $\Delta p(x, Re_w) / \Delta p(x, Re_w = 0)$, where pressure drops are calculated as $\Delta p(x, Re_w) = p(x, Re_w) - p(x = 0, Re_w)$. Parameters used: h = 1 mm, Θ = 0.2, ρ = 1000 kg/m^3, $\mu = 8.55 \cdot 10^{-4}$ Ns/m^2 (water). In figure a) u_m^0 =1 m/s and in b) u_m^0 =10 m/s.

$$p(x,\lambda = L) - p(x,\lambda = 0) = \Im_y h - \frac{1}{2} v_w^2 \rho$$

By denoting the external force as gravity, $\Im_y = \rho g$, the above equation can be given as

$$p(x,\lambda = L) - p(x,\lambda = 0) = \rho h v_w \left(\frac{g}{v_w} - \frac{1}{2} \frac{v_w}{h} \right)$$

For the flux through porous substances usually $|v_w| << 1\ \mathrm{m/s}$ and $\left| \frac{v_w}{h} \right| \leq 1\ \mathrm{s}^{-1}$. Then $\left| \frac{g}{v_w} \right| >> \left| \frac{1}{2} \frac{v_w}{h} \right|$ and $p(x,\lambda = L) - p(x,\lambda = 0) \approx \rho g h$. Thus, if gravity exists, it dominates the pressure difference between the permeate and solid walls.

6. Discussion and conclusions

A perturbation solution for laminar steady state incompressible flow inside permeable and impermeable walls is given. The viscosity and the permeate flux through the porous wall are assumed as constant. The velocity profiles are derived up to a second order solution.

The accuracy of the assumption of constant permeate flux condition Eq.(6b) depends on, for example, pressure or concentration distribution at the porous wall. Large differences at the wall will impair the assumption. If the flux depends only on the pressure variations over the porous wall, as described by, for instance, the Darcy's law, we can study the accuracy of the assumption from the pressure distribution Eq. (37). To study the permeate fluxes in laboratory systems so that v_w is constant, we should avoid the wrong direction of flows. Parallel-flow and counter-flow arrangements inside two channels of different pressure are illustrated in Fig. 5. The channels are separated by a porous wall. The permeate flux through the porous wall depends on the difference between the pressure at the high pressure surface and low pressure surface. Due to pressure losses, the pressure inside the channels is always highest at the inlet of the channels. In a counter-flow arrangement, the permeate flux

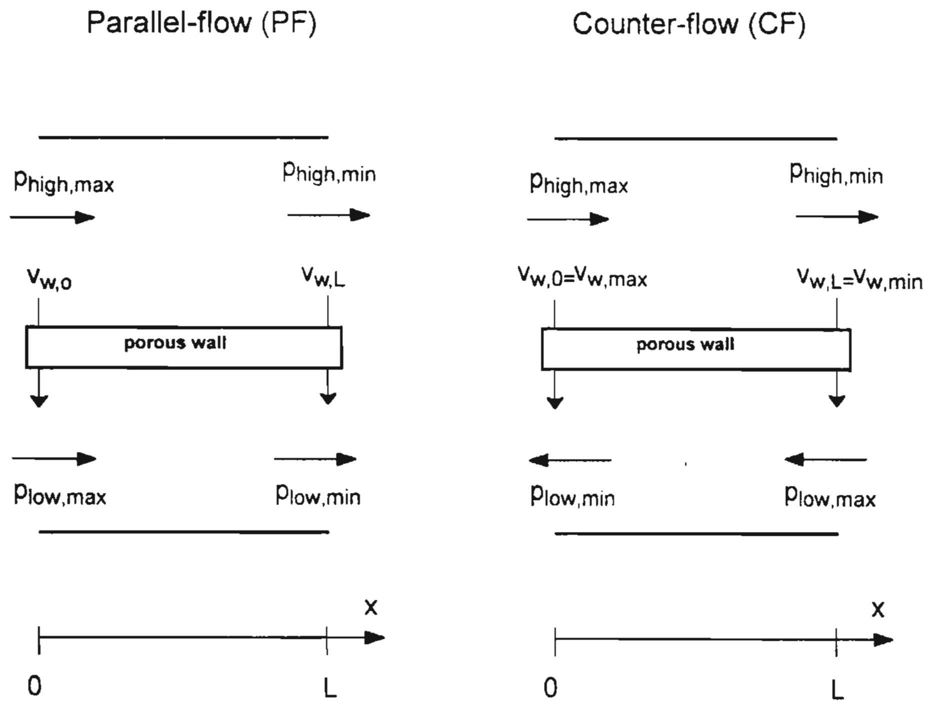

Figure 5. Parallel- and counter-flow arrangements affected by a permeate flux through a porous wall caused by a pressure difference.

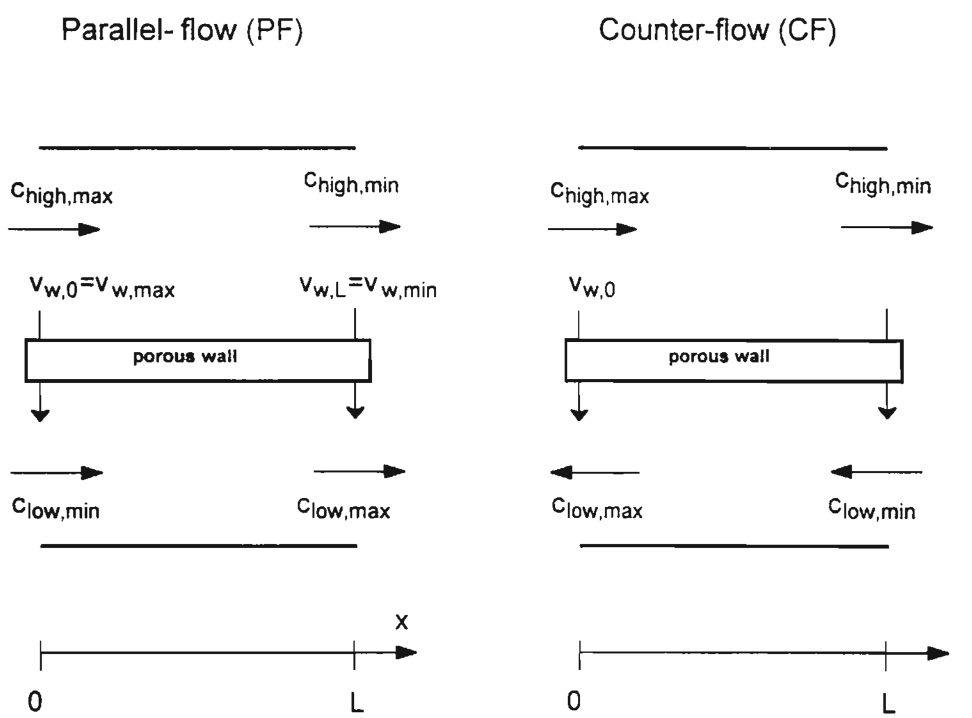

Figure 6. Parallel- and counter-flow arrangements affected by a concentration difference driven permeate flux through a porous wall.

will be maximal at the inlet of the high pressure side and minimal at the outlet position of the high pressure side. Therefore, the differences in the permeate flux will be maximal with the counterflow arrangement. If the pressure losses inside the channels are significant and the pressure difference is the dominant driving force for the permeating flux, the counter-flow arrangement should be avoided.

A similar system is described in Fig. 6 except that the permeate flux depends on the concentration difference between the porous wall in the high concentration channel and low concentration channel. As the permeating flow is directed out from the high concentration side, the concentration in that channel is highest at the inlet and lowest at the outlet. The concentration at the low concentration side, on the other hand, increases after the inlet. That will cause, for parallel flow arrangement, the permeate flow to be maximal at the inlet and minimal at the outlet. Thus, the parallel flow arrangement causes maximal differences in permeate flux and should be avoided if the concentration difference is the dominant driving force.

The study is limited to small absolute values of Reynolds wall numbers, that means to small permeating fluxes through the porous wall or a small distance between the walls. However, in the present study the perturbation treatment does not limit the magnitude of the flow parallel to the walls. Thus, the theory can describe considerable changes in flow velocities in the x-direction if the flow is initially diminutive or the wall is long enough. If the inlet flow velocity is large in the x-direction, it can be approximated as fully developed. However, irrespective of the magnitude of the velocity in x-direction, the velocity profile in the direction perpendicular to the walls is needed when estimating concentration profiles inside a mixture flow.

For wall Reynolds numbers $Re_w \ll 1$, the first order approximation is sufficient. For values $Re_w \ll 0.01$ even the zero order approximation can be applied. If values close to Re_w are studied, a higher order solution may be needed. However, it is not completely certain that the series converge at $Re_w = 1$ or little below.

The solution for the pressure change perpendicular to the channel walls is also solved. This solution can not be found from [1]-[2]. In addition, an external force term perpendicular to the permeable wall is included in the study. Due to some mathematical simplifications the external force term does not affect the velocity profiles. It has an influence only on the pressure profile perpendicular to the porous wall. Under the effect of gravitational force, it is shown that the pressure difference between the permeate and solid wall is usually governed by gravity. The effect caused by the permeate flux is minute.

References

[1] Berman, Abraham, S.: Laminar flow in Channels with porous walls, Journal of Applied Physics (1953), 24, no. 9, 1232-1235.

[2] Chellam, S., Wiesner, M.R., Dawson, C.: Slip at a uniformly porous boundary: effect on fluid flow and mass transfer, Journal of Engineering Mathematics (1992), 26, 481-492.

[3] Beavers, G.D., Joseph, D.G.: Boundary condition at a naturally permeable wall, Journal of Fluid Mechanics (1967), vol. 30, part 1, 197-207.

[4] Saffman, P.G.: On the boundary condition at the surface of a porous medium, Studies in Applied Mathematics (1971), vol.1 no. 2, 93-101.

[5] Nayfeh, Ali, Hasan: Perturbation methods, John Wiley & Sons, New York, 1973.